Engineering and Technology Journal
Journal homepage: engtechjournal.org

Investigation of Thickness Distribution Variation in Deep Drawing of Conical Steel Products

Muhsin J. Jweeg [a], **Adnan I. mohammed** [b], **Mohammed S. Jabbar** [c*]

[a] College of Technical Engineering, Al-Farahidi University, Baghdad, Iraq, muhsin.jweeg@uoalfarahidi.edu.iq

[b] Department of Production Engineering and Metallurgy, University of Technology, Baghdad, Iraq, 70058@uotechnology.edu.iq

[c] Department of Production Engineering and Metallurgy, University of Technology, Baghdad, Iraq, 70226@uotechnology.edu.iq

*Corresponding author.

Submitted: 30/10/2020 Accepted: 27/12/2020 Published: 25/04/2021

K E Y W O R D S

Thickness distribution, conical products, numerical simulation, deep drawing, thinning, steel sheets.

A B S T R A C T

This study investigates the thickness variation behavior of deep drawing conical products under the effect of different forming parameters such as die wall inclination angle, punch velocity, sheet thickness, and sheet metal type. Two types of sheet metal were used, low carbon (AISI 1008) and galvanized steel sheets, of 110 mm diameters circular blanks at 0.9 and 1.2mm thickness formed by tooling set (punch, die, and blank holder). The conical dies inclination angles were at 70º, 72º, and 74º where, the punch velocity was 100, 150, and 200 mm/min. Numerical simulation was conducted using ABAQUS 6.14 where a dynamic explicit solver was used to perform forming of conical products. The results show that maximum thinning occurs at punch nose radius region and maximum thickening in sidewall region and thinning are increased with the increasing of die sidewall angle and sheet thickness. In regard to sheet type, the Lankford coefficients r-value shows a great role in thinning behavior with respect to rolling (r-values direction). The results have shown a good agreement between experimental and numerical work with a maximum discrepancy of 5%.

How to cite this article: M.J. Jweeg, A.I. Mohammed, and M.S. Jabbar, "Investigation of Thickness Distribution Variation in Deep Drawing of Conical Products, "Engineering and Technology Journal, Vol. 39, Part A, No. 04, pp. 586-598, 2021.
DOI: https://doi.org/10.30684/etj.v39i4A.1908

1. INTRODUCTION

The tooling set included a punch that used to push the circular blank to flow into the gap confined between the punch and die. As a result, the circular blank fabricated into conical, cylindrical, or boxshaped products taking the shape of the tooling set with low material west. The typical tooling set of deep drawings is shown in Figure 1. Deep drawing can be classified into two categories: pure drawing and ironing drawing. Pure drawing is a drawing process without a change in the thickness of the original blank, while ironing is a drawing process associated with a reduction in the thickness of the original blank. In sheet metal fabrication bending and stretching are the primary or dominant mechanisms in-plane stress circumstances, and anisotropy, residual stress, and spring back are regarded as important factors. On the other hand, steel is more desirable because of its high strength and strain hardening during forming operations. The material strength increased after forming and ductility decreased [1]. The material becomes thicker in the region where sheet metal loses contact with the punch (punch radius) and thinner in the regions where stresses are higher [2].

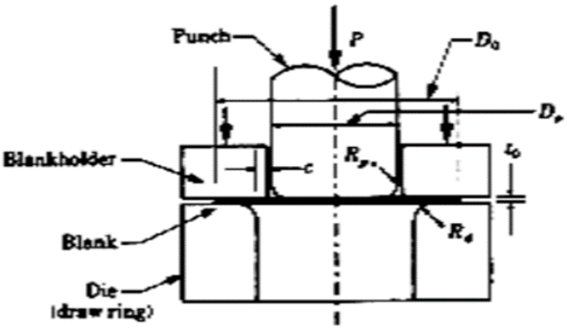

Figure 1: Deep drawing tooling set [1].

Thickness distribution considered one of the important quality criteria in sheet formed products. After deep drawing the thickness is not equally distributed in the formed part. Typically, thickness uniform at punch bottom region, less than the original thickness at punch radius and sidewall near punch radius region and higher than the original thickness at flange region. The presence of thickness distribution after forming can cause a concentration of stresses which cause speeding of damage mechanism in the formed part. So, it is critical to obtain thickness variation during deep drawing since failure by thinning may occur in the deep drawing products [3]. The most common types of defects that can be noted in the deep drawing are wrinkling, thinning, and fracture these defects are related to product safety and performance. In addition, grain size and annealing are important parameters in drawing to enhance the quality of the part, wrinkle pattern, forming load formability, forming limit diagram, and limit drawing ratio [4]. Sherbiny et al. [5] demonstrate the effect of a die and punch radius on residual stresses and thinning of sheets in deep drawing experimentally. Spring back, thinning and thickness distribution of sheet metal in deep drawing operation are predicted by Zein et al. [6]. Zoesch et al. [7] reveal the material to crack and thinning through a deep-drawing operation. H. Zein et al. [8] claimed that using finite element simulation of the deep-drawing process and specify the values of thickness distribution variation will minimize the cost of production due to saving production time and material. The die and punch profile radius are depending on sheet thickness so it is necessary to optimize the die and punch radius. Most defects in the deep-drawing process rely commonly on process parameters: geometry, type of the material, etc. also experimental optimization required expensive and long-time trials. So, numerical and mathematical approaches of optimization are becoming more favorable to predict forming problems in sheet metal forming operations [9-14]. Hu et al [15] used ABAQUS finite element simulation to evaluate thickness variation along with radial and circumferential directions. Padmanabhan [16] study the influence of three of the most important deep drawing parameters named holding force, friction coefficient, and die radius on the thickness distribution of the product. The effect of holding force on thickness of aluminum alloy sheets during the deep drawing process was studied using FEM and experiments by Demirci et al. [17]. According to Demiric study, the experimental and numerical results of product wall thickness distribution demonstrated high agreement.

In this work, the thickness variation behavior of deep drawing conical steel products is investigated under the effect of different forming parameters such as die wall inclination angle, punch velocity, sheet thickness, and sheet metal type. This is achieved experimentally and numerically using the finite element technique.

2. Experimental Work

I. Materials and Mechanical Properties

Two types of sheet metal were used in this study are low carbon and galvanized steel sheets of thickness 0.9 and 1.2 mm. Circular blank rods 110 mm were machined from the steel sheets as work specimens in the forming operation along with a set of tensile specimens by water jet machine in order to characterize the mechanical properties of the materials used and archive high accurate finite element simulation. The tensile test specimens fabricated, according to ASTM standard E8M specification, with respect to the rolling direction: 0^o to the rolling direction, 45^o diagonal to the rolling direction, and transverse to the rolling direction (90^o) as can be seen in Figure 2.

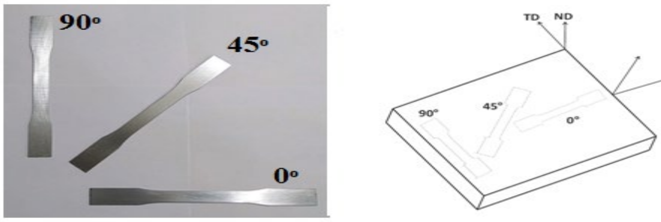

Figure 2: Tensile test specimens according to the rolling direction.

Figure 3 illustrates the relation between true stress-true strain for the two materials after the tensile test was conducted and TABLE I represent the mechanical properties of the materials that obtained experimentally and used in this study. Another group of tensile test specimens, from the two materials chosen to conduct this study, are prepared to measure the level of plastic anisotropy. The specimens are cut parallel, diagonal, and perpendicular to the rolling direction. TABLE II represents the values of the anisotropy coefficient along with normal and planar anisotropy for the two materials with respect to the rolling direction.

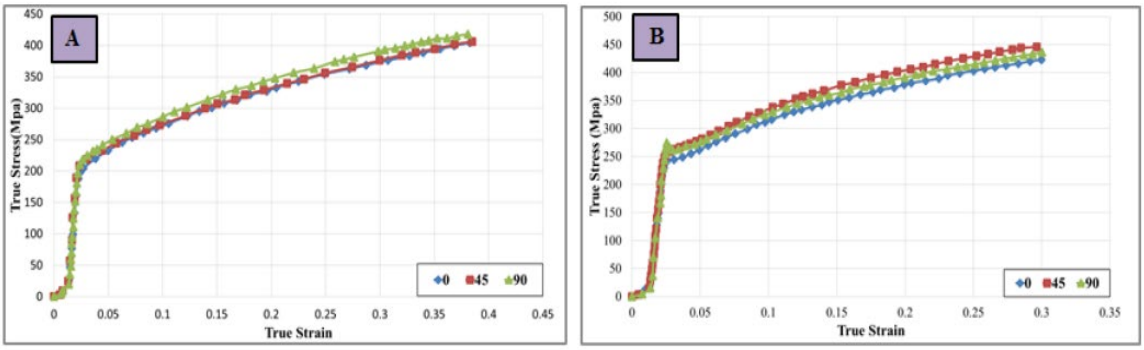

Figure 3: The relationship between true stress- true strain curves along with different angles to the rolling direction for A) low carbon steel and B) galvanized steel.

TABLE I: Mechanical properties of low carbon steel and galvanized steel at different angles with respect to the rolling direction.

Material	Rolling Direction	Yield Strength (MPa)	Tensile Strength (MPa)
Low carbon steel	0^o	205	376
	45^o	211	385
	90^o	218	411
Galvanized steel	0^o	243	407
	45^o	253	444
	90^o	263	431

TABLE II: The values of anisotropy coefficient r_0, r_{45}, and r_{90} at 0°, 45°, and 90° from the rolling direction also the values of normal ($\bar{r}$) and planar (Δr) anisotropy for low carbon steel and galvanized steel.

Material	r_0	r_{45}	r_{90}	$\bar{r}$	Δr
Low carbon steel	0.37583	0.29023	0.5343	0.37265	0.164835
Galvanized steel	0.40092	0.2534	0.4719	0.345	0.18301

II. Tooling and equipment

Three conical punches and dies, of inclination angles 70°, 72°, and 74°, were used to draw circular blanks of 110 mm at the thickness of 0.9- and 1.2-mm. punches and dies designed to handle more than one thickness, which means that one punch and die can be used to draw blanks of 0.9- and 1.2-mm thickness. Punches and dies were made of St.37 tool steel using CNC turning machine and punch and die profile radius kept constant, the value of punch profile radius and die profile radius are 9 and 11 mm, respectively, for all punches and dies (70°, 72°, and 74°) Figure 4 demonstrates the drawing set arrangement while Figure 5 shows punches and dies used in this study.

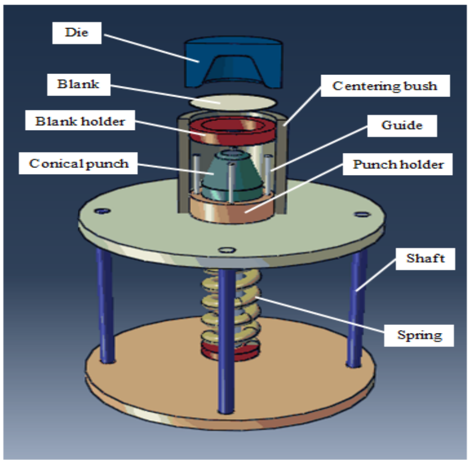

Figure 4: Schematic demonstrating the arrangement of drawing system various components used in this study.

Figure 5: Photograph shows the punches and dies used in this study.

III. Deep Drawing Operation

The drawing experiments were conducted using a WDW200E testing machine, 200 KN maximum loading capacity, associated with a computerized control unit which plots the material behavior during the deformation process as a load-displacement curve. The drawing operation conducted at three punch velocities 100, 150, and 200 mm/min in order to study the effect of punch velocity on the behavior of a spring back the experiments were designed using Minitab 18 software package using the full factorial method. Figure 6 shows fully drawn conical products of various die wall angles, material types, punch velocities, and sheet thickness.

Figure 6: Photographs show the cups produced from different die wall angles, punch velocities, material types, and sheet thicknesses.

3. Numerical Simulation

I. Materials and Mechanical Properties

ABAQUS 6.14 was used to analyze and simulates the deep drawing process and prediction of thickness distribution behavior in conical products. TABLE III demonstrates the mechanical properties of both materials used in finite element simulation and the values of stresses and strains used in the simulation are from true stress-true stain curves that obtained experimentally.

TABLE III: Mechanical properties of the materials used in finite element simulation.

Material	Property	Value
Low Carbon Steel	Young’s modulus	200 GPa
	Density	7.8 g/cm^3
	Poisson ratio	0.3
	Yield stress	205 MPa
Galvanized Steel	Young’s modulus	210 GPa
	Density	7.85 g/cm^3
	Poisson ratio	0.29
	Yield stress	243 MPa

The model in this study has four components are: punch, die, blank, and blank holder where the punch, die, and blank holder defined as rigid bodies and the blank defined as deformable-body figure 8 demonstrate the model generated using ABAQUS 6.14 pre-processor. Rigid bodies (punch, die, and blank holder) meshing using R3D4 and R3D3 elements these elements are specified for rigid bodies and the global size value is 3. In the case of deformable-body (blank), it was meshed using C3D8R and C3D6 elements these types of elements are known as 8-node and 6-node 3D reduced integration elements where sweep technique was utilized in meshing as shown in Figure 7.

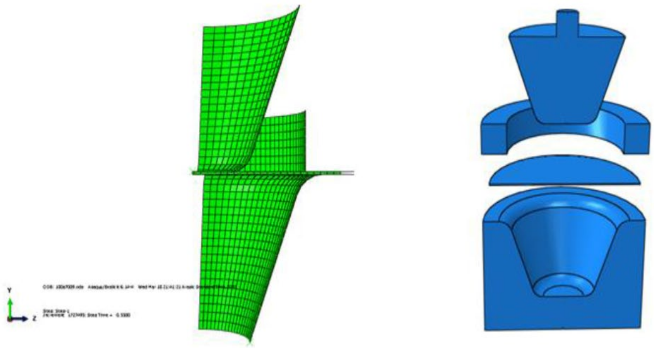

Figure 7: Assembled model meshed using ABAQUS 6.14.

II. Contact and Loading

In order to achieve effective contact modeling of the interaction of rigid and deformable parts a surface-to-surface dynamic explicit contact with finite "sliding penalty" based contact algorithm was used- Associated with three contact pairs: punch-top blank, holder-top blank and die-bottom blank. The coefficient of friction between the interacted surfaces is assumed to be 0.1 for holder-top blank and die-bottom blank contact pairs and 0.15 for punch-top blank contact pairs. The loading consists of three steps the first step is called the initial step where the boundary condition is implemented the second step represents the application of holding force while the third step represents the actual drawing process. The resulting products show a good agreement with experimental work. Figure 8 illustrates the final products from experimental and simulation processes.

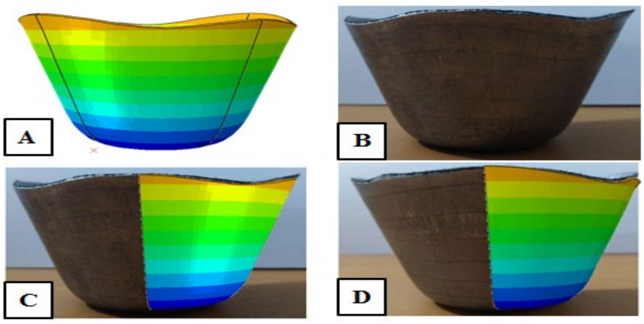

Figure 8: (A) And (B) Products obtained from simulation and experimental work respectively, (C) and (D) represent the agreement between the simulation and experimental work.

III. Thickness Distribution Measurement

in order to measure the thickness distribution along with the rolling, diagonal, and transverse directions one-quarter of the cup had been cut using a water jet machine and the thickness measured at the intersection points between concentric circles and straight lines in the grid using three digits taper tip digital micrometer.

4. RESULTS AND DISCUSSION

Before starting it is very important to state the effect of the Lankford Coefficient (r-value) for the material on thickness distribution. Lankford Coefficient has a great impact on material behavior during the forming process and it is considered as a function of the angle from the rolling direction of the used sheet. So, the r- value is not constant in all directions, but it has different values according to the rolling direction. To demonstrate the effect of r- value, low carbon steel material that has r-values of r_0, r_{45}, and r_{90} are 0.37583, 0.29023, and 0.5343 respectively with 70^o die wall angle was taken as an example from this study during the deep-drawing process. Hill's model was used to show the effect of the Lankford coefficient in finite element simulation because this criterion takes the r-value into the account. Figure 9 shows the deformed cup divided into different regions (A) sidewall region, (B) punch corner region and, (C) cup bottom region. The effect of r- value for 0^o, 45^o, and 90^o directions demonstrated in Figure 10 it can be noted from the figure that small thinning occurs at region (C) then thinning increase at region (B) more thickening become obvious at a region (A). The thinning at regions (B) and (C) has a maximum value for 90° and minimum for 45° from the rolling direction. It can be concluded that thickness increase with r- value decrease which means that the material part in the direction having a lower value of r flow faster than the part having a higher r-value and the thickening at cup rim will be higher, for this study the 45° cup direction represent this fact. In this section, we will use % thinning to demonstrate the relation between reduction in thickness with different forming variables since thinning is a major defect and the product considered a failure if exceed 20% from thickness. The thinning percentage can be obtained from the following equation:

$$\%\,thinning = \frac{\text{original thickness} - \text{thickness after deformation}}{\text{original thickness}} \times 100\% \quad (1)$$

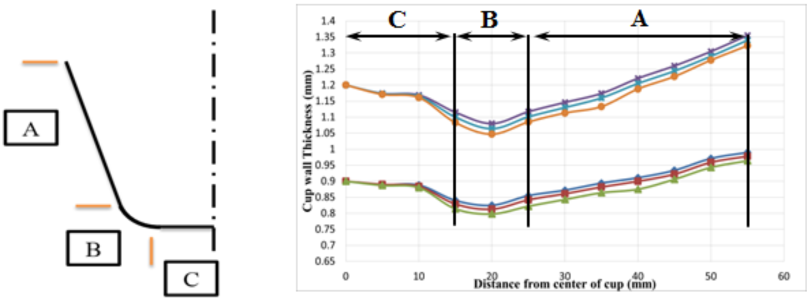

Figure 9: Different regions of deformed part.

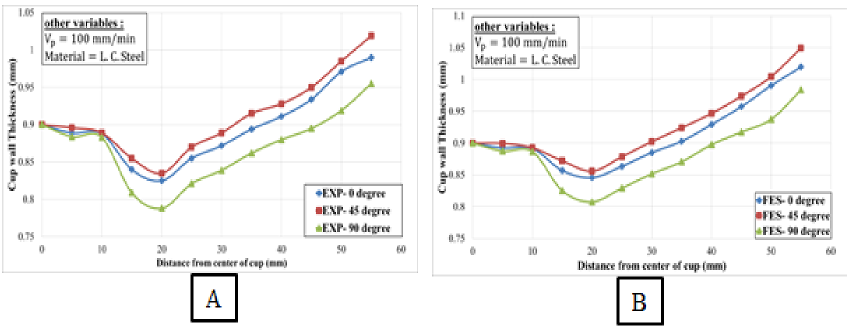

Figure 10: The effect of r- value on thickness distribution A) EXP and B) FES along 0°, 45° and, 90° directions.

Thinning increased with increasing die wall angle. Higher thinning can be seen in the punch corner region (region B) for dying with 74° wall angle this may return to the geometrical design of the die where the punch stroke is set constant at 55 mm and die bottom diameter at 40 mm plus die clearance for all dies as productive in experimental work. This means when decreasing the die wall angle, the die opening will increase. From that, it was concluded that decreasing die wall angle causes increasing in die opening and the sheet region confined between the blank holder and die become smaller leading to less contact area and less tensile and blank holding forces resisting drawing load which, minimized stretching in cup wall consequently lower thinning in cup wall thickness. Figures 11, 13, and 15 show the relation between thickness behavior and die wall angle for low carbon steel and Figures 12, 14, and 16 for galvanized steel while Tables IV and V demonstrate the value of thinning at various variables with different forming conditions experimentally and numerically. Punch velocity has a slight effect on thickness distribution behavior as seen from thinning values in Tables IV and V. Increasing punch velocity shows a very small increase in thickness reduction the cause of this can be attributed to frictional conditions during forming operation and strain hardening phenomenon which increase rapidly with velocity increasing and since the area of contact in deep drawing of conical cups are less than that for straight-walled cups, the effect of punch velocity on thickness distribution will be lower also and its effect are mainly limited at punch corner region with slight decreasing or increasing according to bunch velocity applied. In regard to the effect of sheet thickness Tables IV and V show the effect of a couple of blank thickness values on thickness distribution as it is noted that the increasing blank thickness of the same material will lead to an increase in thinning percentage. Also, the average distribution of thickness of the blank will increase with increasing of its thickness. This increase in thinning for higher thickness return to the fact that thicker blanks can be gripped tightly than thinner blanks during the forming process, on the other hand, a thicker sheet is softer due to an increase in volume, which means it can be stretched to a higher extent leading to magnifying the thinning in the produced cup. While, the behavior of thickness distribution for different materials shows that the value of thinning is higher along rolling direction (0^o) for galvanized steel than low carbon steel, but for diagonal and transverse (45^o and 90^o respectively) to rolling direction it can be seen that thinning lower for galvanized steel than low carbon steel the reason for that depend mainly on the r-value of material for each part and its angle along with cup with respect to the rolling direction for low carbon steel the value of r_0, r_{45}, and r_{90} are 0.37583, 0.29023, and 0.5343 respectively and for galvanized steel, the value of r_0, r_{45}, and r_{90} are 0.40092, 0.2534, and 0.4719 respectively, and as mentioned earlier the ability of the part of the material to flow increased with decreasing of r-value, as a result, the thinning decrease with decreasing of r-value for the part of the material.

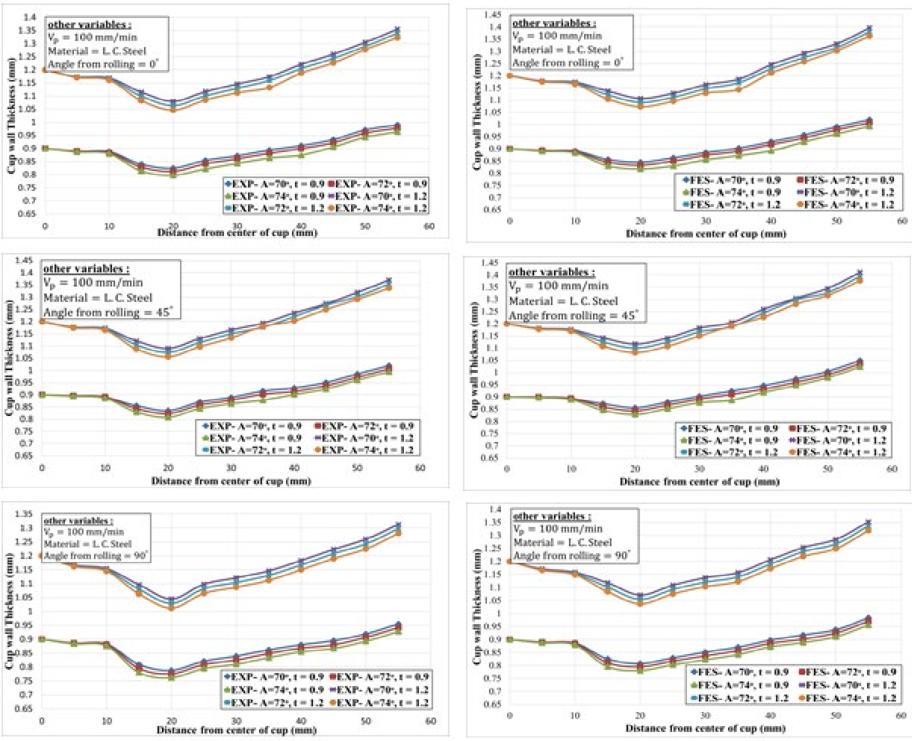

Figure 11: Effect of die wall angle variation in thickness behavior of low carbon steel at 100 mm/min punch velocity and 0.9 &1.2 mm thickness along 0^o, 45^o and, 90^o directions experimentally and numerically.

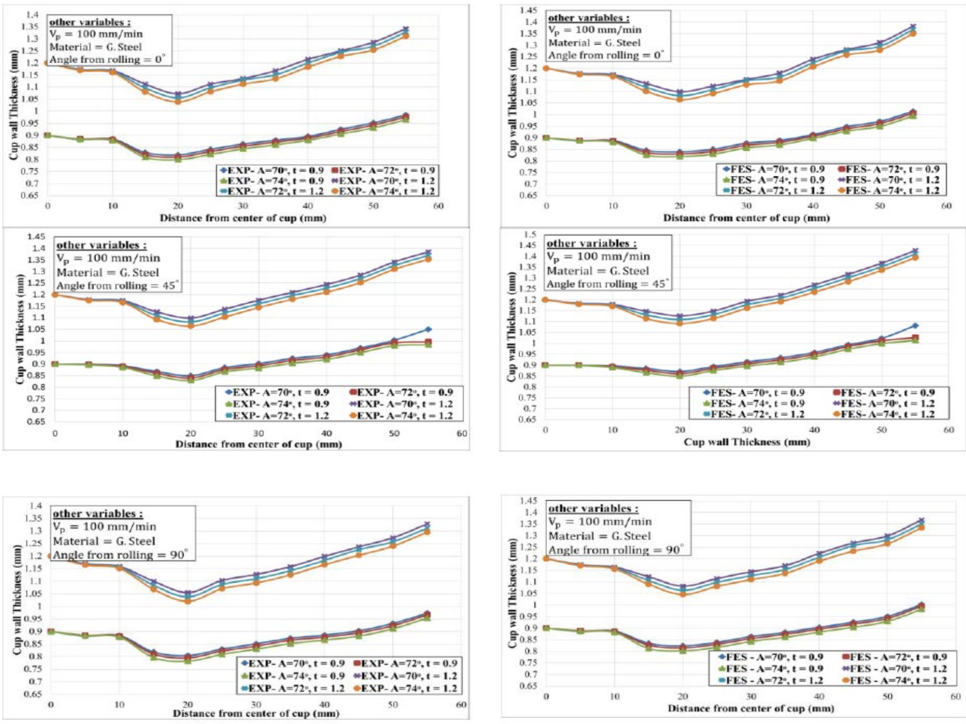

Figure 12: Effect of die wall angle variation in thickness behavior of galvanized steel at 100 mm/min punch velocity and 0.9 &1.2 mm thickness along 0°, 45° and, 90° directions experimentally and numerically.

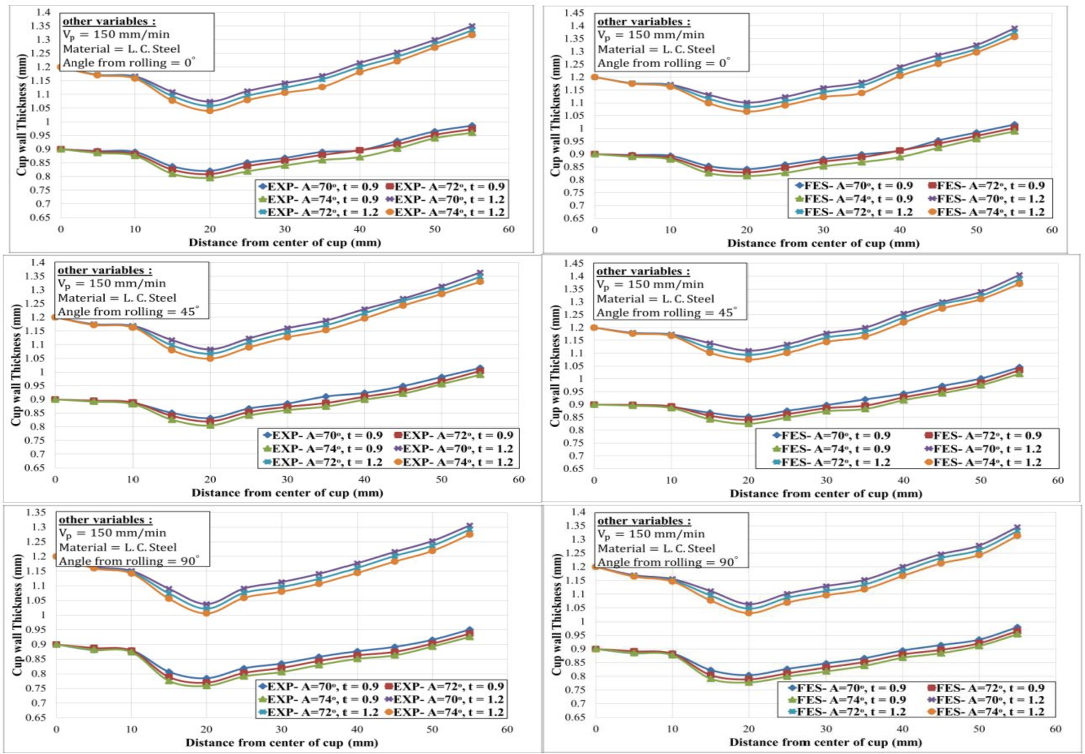

Figure 13: Effect of die wall angle variation in thickness behavior of low carbon steel at 150 mm/min punch velocity and 0.9 &1.2 mm thickness along 0°, 45° and, 90° directions experimentally and numerically.

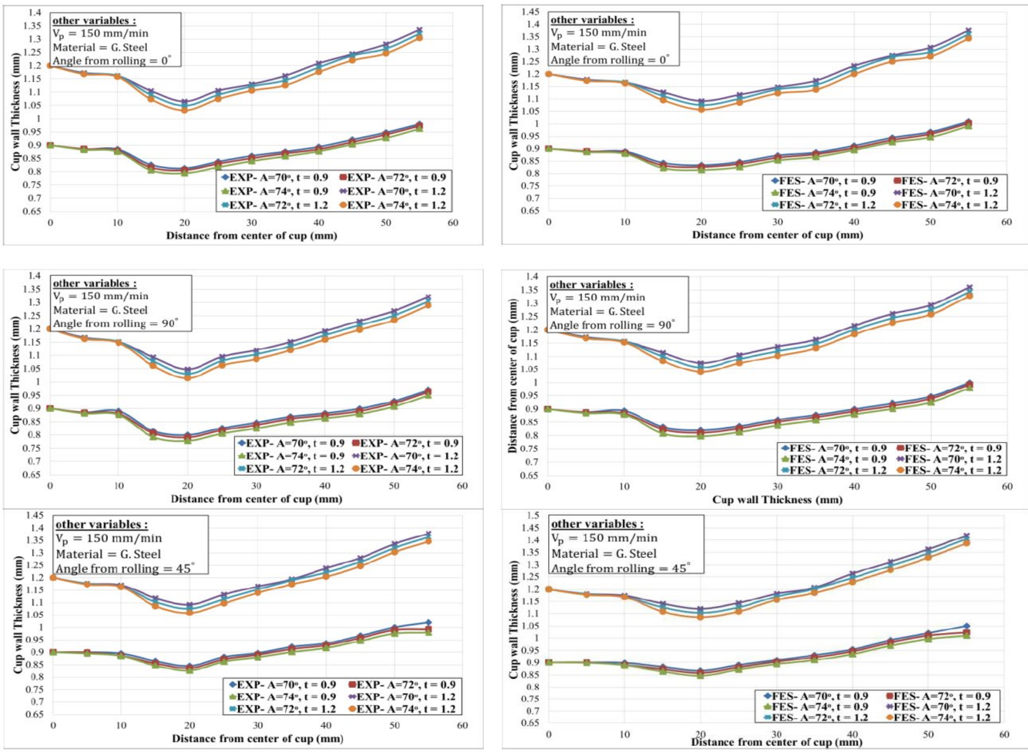

Figure 14: Effect of die wall angle variation in thickness behavior of galvanized steel at 150 mm/min punch velocity and 0.9 &1.2 mm thickness along 0°, 45° and, 90° directions experimentally and numerically.

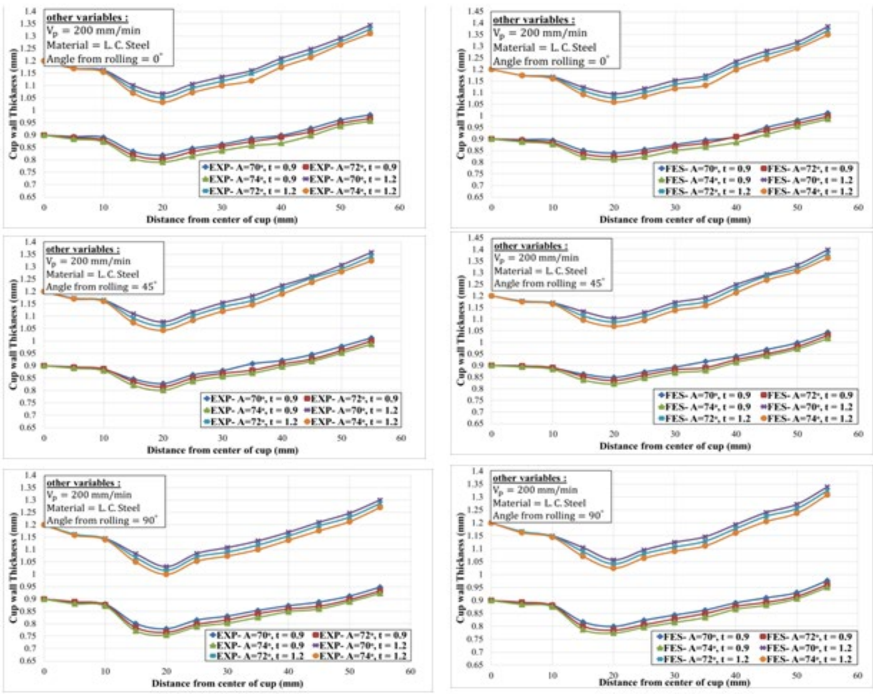

Figure 15: Effect of die wall angle variation in thickness behavior of low carbon steel at 200 mm/min punch velocity and 0.9 &1.2 mm thickness along 0°, 45° and, 90° directions experimentally and numerically.

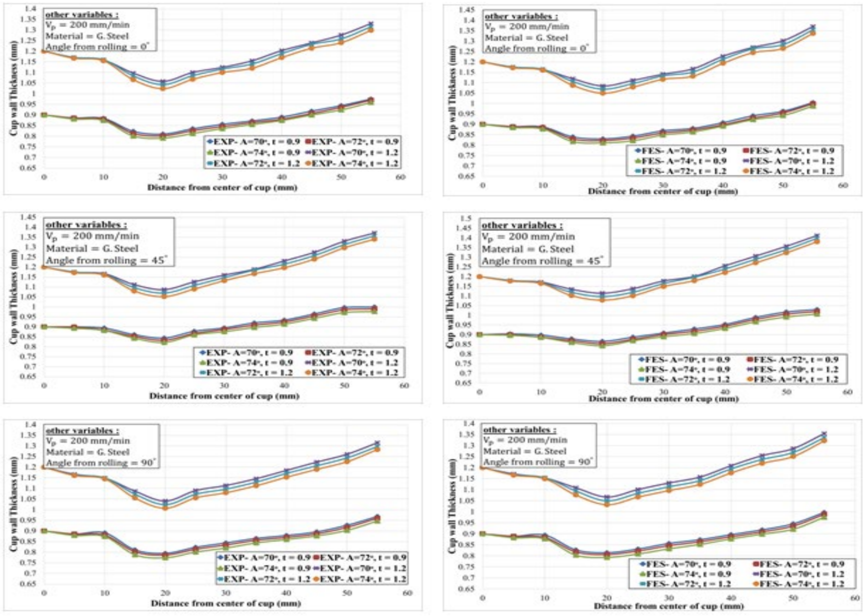

Figure 16: Effect of die wall angle variation in thickness behavior of galvanized steel at 200 mm/min punch velocity and 0.9 &1.2 mm thickness along 0°, 45° and, 90° directions experimentally and numerically.

TABLE IV:%thinning values obtained experimentally.

% Thinning - EXP						
Material Type	*Sheet Thickness (mm)*	*Die wall angle (°)*	*Angle from the rolling direction (°)*	*Punch Velocity (mm/min)*		
				100	*150*	*200*
Low Carbon Steel	0.9	70°	0°	8.333	8.778	9
			45°	7.222	7.556	8
			90°	12.444	12.78	13.33
		72°	0°	9.667	10.111	10.67
			45°	8.556	8.889	9.44
			90°	13.778	14.44	14.89
		74°	0°	11.333	11.667	12.11
			45°	10.222	10.556	11
			90°	15.333	15.67	16.11
	1.2	70°	0°	10	10.5	11
			45°	9.167	9.75	10.25
			90°	12.917	13.5	14.08
		72°	0°	11.333	11.833	12.33
			45°	10.5	11.083	11.58
			90°	14.25	14.83	15.33
		74°	0°	12.75	13.333	13.92
			45°	12	12.583	13.08
			90°	15.667	16.17	16.67
Galvanized Steel	0.9	70°	0°	9	9.67	10
			45°	5.56	6	6.22
			90°	10.67	11.11	11.67
		72°	0°	10	10.44	10.89
			45°	6.67	7	7.44
			90°	11.67	12.11	12.56
		74°	0°	11.22	11.78	12.11
			45°	7.89	8.22	8.67
			90°	13.11	13.56	14
	1.2	70°	0°	10.67	11.25	11.83
			45°	8.42	9	9.42
			90°	12.08	12.67	13.25
		72°	0°	12.08	12.58	13.08
			45°	9.83	10.33	10.83

		90°	13.5	14.08	14.67
	74°	0°	13.5	14.08	14.67
		45°	11.33	11.75	12.33
		90°	15	15.5	16.08

TABLE V: %thinning values obtained from simulation

% Thinning - FES						
Material Type	***Sheet Thickness (mm)***	***Die wall angle (°)***	***Angle from the rolling direction (°)***	***Punch Velocity (mm/min)***		
				100	**150**	**200**
Low Carbon Steel	0.9	70°	0°	6.042	6.497	6.73
			45°	4.903	5.244	5.7
			90°	10.256	10.6	11.17
		72°	0°	7.408	7.864	8.43
			45°	6.269	6.611	7.18
			90°	11.622	12.31	12.76
		74°	0°	9.117	9.458	9.91
			45°	7.978	8.319	8.78
			90°	13.217	13.56	14.01
	1.2	70°	0°	7.75	8.263	8.78
			45°	6.896	7.494	8.01
			90°	10.74	11.34	11.94
		72°	0°	9.117	9.629	10.14
			45°	8.263	8.86	9.37
			90°	12.106	12.7	13.22
		74°	0°	10.569	11.167	11.76
			45°	9.8	10.398	10.91
			90°	13.558	14.07	14.58
Galvanized Steel	0.9	70°	0°	6.73	7.41	7.75
			45°	3.19	3.65	3.88
			90°	8.43	8.899	9.46
		72°	0°	7.75	8.21	8.66
			45°	4.33	4.68	5.13
			90°	9.46	9.91	10.37
		74°	0°	9	9.57	9.91
			45°	5.59	5.93	6.38
			90°	10.94	11.39	11.85
	1.2	70°	0°	8.43	9.03	9.63
			45°	6.13	6.73	7.15
			90°	9.89	10.48	11.08
		72°	0°	9.89	10.4	10.91
			45°	7.58	8.09	8.6
			90°	11.34	11.94	12.53
		74°	0°	11.34	11.94	12.53
			45°	9.12	9.54	10.14
			90°	12.88	13.39	13.99

5. CONCLUSIONS

1) The results show good agreement between experimental and numerical work with a maximum discrepancy of 5%.

2) Thinning increased with the increasing of die wall angle due to geometrical differences where the die opening increased with decreasing of die wall angle leading to reduce the area to hold by a blank holder which reduces stretching during forming at constant die bottom diameter and constant punch displacement.

3) Punch velocity has a small effect on thickness distribution behavior where the thickness reduction increases with the increase of punch velocity and this may return to frictional conditions and strain hardening phenomenon occur during velocity increasing.

4) Thinning increased with the increase of sheet thickness the main reason for that is the thicker the sheet softer it becomes and the higher the thickness of the sheet more tightly it gripped by the blank holder.

5) The thinning for different types of sheets depends on the values of Lankford coefficients the lower r-values the lower the thinning becomes.

References

[1] K. Lange, Hand book of metal forming, university of Stuttgart, McGraw-Hill Book Company, 1st edition, Michigen, U.S.A, 1985.

[2] Y. N. Dhulugade, P. N. Gore, Design and development of sheet metal draw component using CAE technology, Int. j. emerg. technol. adv. Eng., 3 (2013.) 30-39.

[3] T. Altinbalik, A. Tonka, Numerical and experimental study of sheet thickness variation in deep drawing processes, Int. J. Mod. Manuf. Technol., 2 (2012) 2067–3604.

[4] M. Kadkhodayana , E. Afshin, Thinning behavior of laminated sheets metal in warm deep-drawing process under various grain sizes, MATEC. Web. Conf., 80 (2016). https://doi.org/10.1051/matecconf/20168015001

[5] M. El Sherbiny, H. Zein, M. Abd-Rabou, Thinning and residual stresses of sheet metal in the deep drawing process, Mater. Des., 55 (2014) 869-879. https://doi.org/10.1016/j.matdes.2013.10.055

[6] H. Zein, M. El Sherbiny, M. Abd-Rabou, Thinning and spring back prediction of sheet metal in the deep drawing process, Mater., 53 (2014) 797-808. https://doi.org/10.1016/j.matdes.2013.07.078

[7] A. Zoesch, T. Wiener, M. Kuhl, Zero defect manufacturing: detection of cracks and thinning of material during deep drawing process, procedia. CIRP. 33 (2015) 179-184. https://doi.org/10.1016/j.procir.2015.06.033

[8] H. Zein, M. El-Sherbiny, M. Abd-Rabou, M. El Shazly, Effect of die design parameters on thinning of sheet metal in the deep drawing process, Am. J. Mech. Eng., 1 (2013) 20-29 . https://doi.org/10.12691/ajme-1-2-1

[9] R. Bahloul, S. Benelechi , Ph. Dal Santo, H. Naceur, Optimization of bending process by means of response surface and moving least squares methods, J. Appl. Math. ., 22 (2006) 25-54.

[10] S. K. Singh, D. R. Kumar, Application of a neural network to predict thickness strains and finite element simulation of hydro-mechanical deep drawing, Int. J. Adv. Manuf. Technol., 25 (2005) 101-107. https://doi.org/10.1007/s00170-003-1842-4

[11] T. Ohata, Y. Nakamura, T. Katayama, E. Nakamachi, Development of optimum process design system for sheet fabrication using response surface method, J. Mater. Process. Technol., 143– 144 (2003) 667–672 . https://doi.org/10.1016/S0924-0136(03)00314-5

[12] T. Jansson, A. Andersson, L. Nilsson, Optimization of draw-in for an automotive sheet metal part: An evaluation using surrogate models and response surfaces, J. Mat. Process. Technol., 159 (2005) 426–434. https://doi.org/10.1016/j.jmatprotec.2004.06.011

[13] L. B. Ayed, C. Robert, A. Delaméziere, M. Nouari, J.L. Batoz , Simplified numerical approach for incremental sheet metal forming process, Eng. Struct., 62-63(2014)75-86.

[14] L. B. Ayed, A. Delamézière, J-L. Batoz, C. Knopf-Lenoir, Prediction of the localized necking phenomena based on the MMFC and optimization of blank holder forces, Int. J. Form. Process., 10 (2007) 277-301. https://doi.org/10.3166/ijfp.10.277-301

[15] J. Hu , J. J. Jonas , T . Ishikawa, FEM Simulation of Deep Drawing of Textured Aluminum Sheets Using Anisotropic Fourth-Order Strain-Rate Potential, Mat. Sci . Eng., 39 (1998) 469-477. https://doi.org/10.2320/matertrans1989.39.469

[16] R. Padmanabhan, M. C. Oliveira, J.L. Alves, L.F. Menezes, Influence of process parameters on deep drawing of stainless steel, Finite Elem. Anal. Des., 43 (2007) 1062-1067. https://doi.org/10.1016/j.finel.2007.06.011

[17] H.I. Demirci, C. Esner, M. Yasar, Effect of the blank holder force on drawing of aluminum alloy square cup: Theoretical and experimental investigation, J. Mat. Pro. Tech ., 206 (2008) 152-160. https://doi.org/10.1016/j.jmatprotec.2007.12.010